

Coarsening of Precipitation Patterns in a Moving Reaction-Diffusion Front

A. Volford¹, I. Lagzi^{2,3}, F. Molnár Jr.⁴, and Z. Rácz⁴

¹*Department of Physics, University of Technology and Economics, 1521 Budapest, Hungary*

²*Department of Meteorology, Eötvös University, 1117 Budapest, Hungary*

³*Department of Chemical and Biological Engineering,*

Northwestern University, Evanston, Illinois 60208, USA and

⁴*Institute for Theoretical Physics–HAS, Eötvös University, 1117 Budapest, Hungary*

(Dated: November 2, 2018)

Precipitation patterns emerging in a 2D moving front are investigated on the example of NaOH diffusing into a gel containing AlCl_3 . The time evolution of the precipitate $\text{Al}(\text{OH})_3$ can be observed since the precipitate redissolves in the excess outer electrolyte NaOH and thus it exists only in a narrow, optically accessible region of the reaction front. The patterns display selfsimilar coarsening with a characteristic length ξ increasing with time as $\xi(t) \sim \sqrt{t}$. A theory based on Cahn-Hilliard phase-separation dynamics including dissolution is shown to yield agreement with the experiments.

PACS numbers: 05.70.Ln,64.60.My,64.75.Xc,82.20-w

Understanding precipitation patterns formed in a moving reaction front is important both from the basic aspect of extending our knowledge of phase separation dynamics and from the point of view of technological applications. Indeed, the formation of precipitation structures, well localized in space and time, underlies the notion of the so called "bottom up" designs [1, 2, 3, 4] where one creates structures directly in the bulk. A natural way of realizing such design is to have a reaction-diffusion process and control the dynamics of the reaction zone i.e. control both the position of the front and the rate of the creation of the reaction product which yields the precipitate provided its concentration exceeds a threshold value.

Recently, there have been several attempts at controlling reaction zones [3, 4, 5, 6] with the most promising results emerging from the use of the ionic nature of the reagents and realizing control through time-dependent electric currents [7]. Although these experiments demonstrate that one can create one dimensional structures reproducibly at the scale of $\sim 500\mu$, the downsizing of the patterns to submicron scales raises several problems related to the front. One of them is the width of the front which obviously restricts the downscaling in the direction of the motion of the front. The second one is related to the inhomogeneities within the front which may lead to unwanted precipitation structures in the plane perpendicular to the motion of the front. The scale of these structures clearly limits downscaling in the transverse direction.

The width of reaction fronts has been extensively studied theoretically [8, 9] as well as experimentally [10, 11, 12] and one has some ideas about the control parameters in this case. Very little is known, however, about the transverse patterns in a moving reaction zone, though bulk coarsening has been studied in connection with the so called gradient-free precipitation experiments [13, 14].

Our aim here is to initiate experimental and theoretical studies of the coarsening dynamics of the transverse patterns in reaction zones. This task is made feasible ex-

perimentally by overcoming the transparency problem in a way suggested by earlier studies of Liesegang type phenomena [15, 16, 17, 18, 19, 20, 21]. Namely, the reaction-diffusion process is set in a nearly transparent gel and, furthermore, appropriately chosen electrolytes are used so that the reaction product undergoes redissolution in the excess of the outer electrolyte. As a result, precipitate exists only in a narrow region restricted to the reaction zone and its time evolution can be followed in detail.

We observed the patterns in the moving reaction zone in an experimental setup detailed below. The visual observations suggested that the system displayed a selfsimilar coarsening and this was quantified through the time dependence of the characteristic lengthscale $\xi(t)$ of the pattern, with the main experimental result being that $\xi(t) \sim \sqrt{t}$. Theoretically, the effective dimensionality of the coarsening system is not entirely obvious, and there are several candidates for driving the coarsening process. We studied this problem by generalizing the Cahn-Hilliard theory of precipitation to include sources and sinks coming from the emergence of the reaction product in the reaction zone, and from the redissolution of the precipitate in the excess outer electrolyte, respectively. The numerical solutions of the equations in three dimension are in agreement with the experimentally observed $\xi(t) \sim \sqrt{t}$. This suggests the natural picture that the sources and sinks are relevant perturbations on the particle conservation, and we observe a curvature driven late-stage coarsening in a model with nonconserved order parameter [22, 23].

In the experiments, a 1 w/w% agarose (Reanal) gel was prepared with height of 0.6 – 0.7 cm in a Petri dish. After the gelation process took place ($\approx 2-3$ h), the inner electrolyte (AlCl_3) was poured on top of the agarose gel to obtain a given concentration in the gel (0.48 mol/L – 0.56 mol/L). After 64 hours the inner electrolyte solution was removed from top of the gel and replaced by the outer electrolyte (NaOH of fixed concentration 2.5 mol/L).

A white precipitation layer formed immediately at the gel interface, and this layer started to move into the gel.

The evolution of precipitation pattern in the moving layer was recorded in reflected light using a EOS-20D camera connected to a computer. Typical recording period was $t = 25$ minutes and we analyzed the processes in this time window supposing that the light intensity is proportional to the precipitation concentration [24].

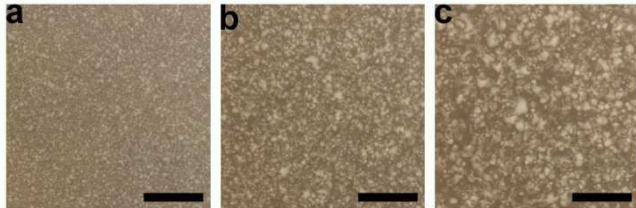


FIG. 1: Time evolution of the precipitation pattern in the reaction zone for the samples with $[\text{NaOH}] = 2.5\text{M}$ (outer electrolyte) and $[\text{AlCl}_3] = 0.52\text{M}$ (inner electrolyte). The front moves perpendicularly to the plane of the picture and the pictures were taken at $t_1 = 180\text{s}$ (a), $t_2 = 480\text{s}$ (b), and $t_3 = 960\text{s}$ (c) after the initiation of the reaction. The length of the scalebars is 1cm.

As shown in Fig.1, the patterns have a random appearance and they coarsen with time. The coarsening displays selfsimilarity as indicated by Fig.2 where the pictures have been magnified by $1/\sqrt{t}$ with t being the elapsed time from the initiation of the process. The selfsimilarity can be quantified by measuring the time evolution of the characteristic length $\xi(t)$ of the precipitation structures. We found ξ^2 through calculating the structure factor of the grayscale values of the pattern and evaluating the average of the wavenumber squared $\xi^2 \sim 1/\langle k^2 \rangle$. The results for three different inner electrolyte concentrations are displayed in Fig.3 and we can see a well defined diffusive growth $\xi^2 \sim 2D_{\perp}t$ regime.

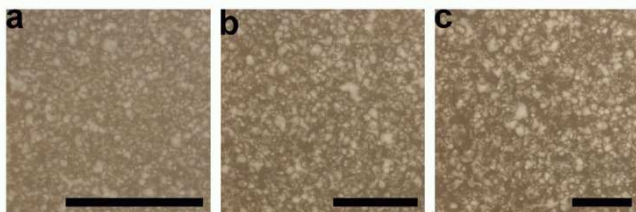


FIG. 2: Visual demonstration of the scaling in the evolution seen in Fig.1. Parts of the panels (a) and (b) are magnified by factors $(t_3/t_1)^{1/2}$ and $(t_3/t_2)^{1/2}$, respectively. The scalebars are the same length of 1cm.

The transverse diffusion coefficient D_{\perp} can be estimated from Fig.3, and we find $D_{\perp} = \xi^2/2t \approx 5 \cdot 10^{-10} \text{m}^2\text{s}^{-1}$. It is remarkable that D_{\perp} is an order of magnitude smaller than the diffusion coefficients of the small hydrated ions.

Our understanding of the observed phenomena is as follows. The hydroxide ion (outer electrolyte) diffuses into the gel, and the white precipitation layer at the gel

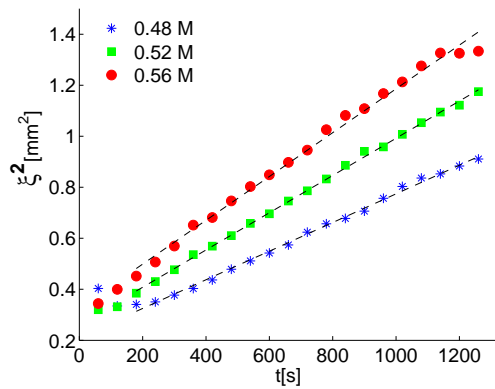
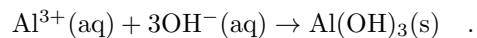
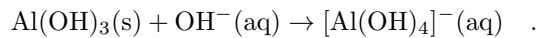


FIG. 3: Square of the characteristic length ξ^2 of the precipitation patterns plotted as a function of time t for three inner electrolyte concentrations and at fixed outer electrolyte concentration ($a_0 = 2.5\text{M}$). We calculated ξ^2 from the 2nd moment of the structure factor of the patterns.

interface is produced by the reaction with the inner electrolyte (aluminum ions)



Next, this layer redissolves due to the complex formation of aluminum hydroxide in the excess of hydroxide ions producing a soluble aluminum complex



The combination of the precipitation and of the complex-formation processes results in a thin precipitation layer moving through the gel. It should be emphasized, however, that the motion is solely the transport of chemical species and not of the precipitate.

Within the above picture, the coarsening in the reaction zone emerges from a complicated interplay of the dynamics of the reaction zone, of the aggregation onto the already present precipitate, and of the redissolution process. As a first step in understanding the interplay of these processes, we approached the problem through coarse grained (mean field) equations by using a model [25] that has been developed in a series of papers during the last decade [7, 18].

The three processes we include are as follows. First, the reaction of the electrolytes $A + B \rightarrow C$ yields the reaction product C . Since the process takes place in a gel, no convection is present and it can be modeled as a simple reaction-diffusion process. This reaction provides the source for the precipitation which is modeled as a phase separation of C s described by the Cahn-Hilliard equation with a source term. Finally, the C 's redissolution in the excess A s (complex formation; $A + C \rightarrow \text{Complex}$) appears as a sink term both in the Cahn-Hilliard equation and in the reaction-diffusion equation for the A s.

The picture can be further simplified if we assume that $A + B \rightarrow C$ is an irreversible process for totally dissoci-

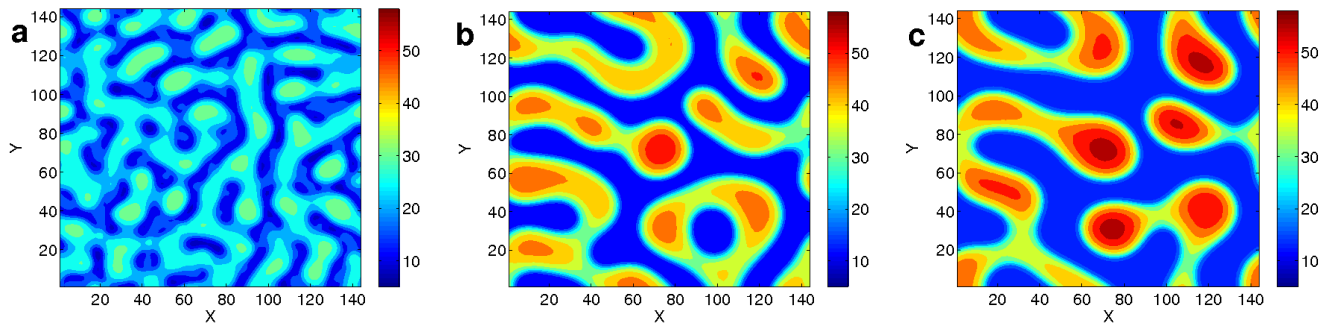


FIG. 4: Simulation results for the spatial distribution of C integrated along the z direction. The parameters used were: $b_0/a_0 = 0.18$, $c_h/a_0 = 0.2$, $c_l/a_0 = 0$, $D = 10^{-9} \text{ m}^2\text{s}^{-1}$, $k_1 = 8.6 \text{ M}^{-1}\text{s}^{-1}$, $k_2 = 0.13 \text{ M}^{-1}\text{s}^{-1}$, $\lambda = 0.83 \times 10^{-9} \text{ m}^2\text{s}^{-1}$, $\sigma = 10^{-6} \text{ m}^2$, the grid spacing and the time step were 0.01 mm and 0.003 s, respectively. The snapshots are taken at 75s, 600s and 1200s.

ated electrolytes A and B , and that the case of monovalent ions with equal diffusion coefficients are considered. Then the equations take the following form:

$$\partial_t a = D\Delta a - k_1 ab - k_2 ac \quad (1)$$

$$\partial_t b = D\Delta b - k_1 ab \quad (2)$$

$$\partial_t c = -\lambda\Delta(\delta f/\delta c) + k_1 ab - k_2 ac + \sqrt{c}\eta. \quad (3)$$

Here D is the diffusion coefficient of the ions, while k_1 and k_2 are the rates of reaction and of complex formation, respectively. We take k_1 to be large resulting in a reaction zone of negligible width (note that this assumption is compatible with the typical reactions used in experimental setups that result in Liesegang structures). The thermal fluctuations in c are described by a noise term $\sqrt{c}\eta$ which conserves the total number of C particles [26]. The free energy (f) underlying the thermodynamics of the phase separation (3) is assumed to have minima at some low (c_l) and high (c_h) concentrations, and it is assumed to be of a Ginzburg-Landau form. Its functional derivative most compactly given in terms of a shifted and rescaled concentration $m = (2c - c_h - c_l)/(c_h - c_l)$

$$\frac{c_h - c_l}{2} \frac{\delta f}{\delta c} = \frac{\delta f}{\delta m} = m - m^3 + \sigma\Delta m. \quad (4)$$

Finally, σ and λ in eq.(3) are setting the spatial- and the time scales. They can be chosen to reproduce the correct time and lengthscales in experiments [27].

The initial conditions to the above equations are set according to the experiments. The outer and inner electrolytes are homogeneously distributed in the lower ($z < 0$) and upper ($z > 0$) halfspaces with concentrations a_0 and $b_0 \ll a_0$, while the initial concentration of C is $c_0 = 0$ everywhere. For solutions in finite rectangular boxes, we applied no-flux boundary conditions at the borders along the z axis while periodic boundary conditions were used at the rest of the border planes.

Equations (1-3) together with (4) were discretized on a uniform 3D grid of size $144 \times 144 \times 704$, and finite-size effects were checked on grids of size $160 \times 160 \times 568$

(no effects were observed) and $96 \times 96 \times 1584$ (effects were seen: the final characteristic length was increased roughly by factor of two).

The resulting ordinary differential equations were integrated in time by Euler method (fast simulations were made feasible by the parallel programming possibilities of video cards [28]). The results from the simulations are summarized in Figs. 4 and 5.

Fig. 4 suggests the existence of two stages in the evolution of the system. There is an initial period when the unstable, homogeneous density of C s produced by the front begins to evolve towards the equilibrium densities (Panel *a* in Fig. 4). This stage is driven by the initial perturbations (noise) which determines whether the concentration in a given neighborhood grows or diminishes.

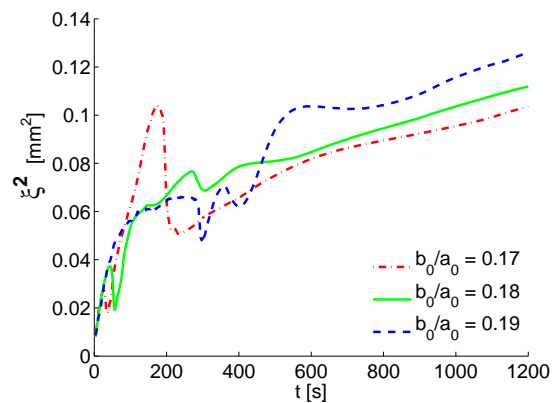


FIG. 5: Simulation results demonstrating the diffusive growth $\xi^2 \sim t$ of the characteristic lengthscale ξ .

The first stage is finished when the high- or low-concentration states are reached in a significant fraction of the system and an initial phase of fast coarsening has also taken already place. The emerging high-concentration regions (Panel *b* in Fig. 4) form a structure which is the base for the next stage, the self-similar coarsening. It should be noted that the memory of this

structure can be recognized throughout the later stages of the coarsening (Panel *c* in Fig. 4).

In order to compare with experiments, we calculated the structure factor and the characteristic length $\xi(t)$ by processing pictures as in case of the experiments. The results for various inner electrolyte concentrations are shown in Fig.5. As we can see, there is a fast initial stage governed by noise and short-scale relaxation to the equilibrium concentrations, followed by the late-stage coarsening. The initial large fluctuations in ξ are due to the fact that, at the initial stage, there is a significant probability for two precipitation bands to coexist. The averaging of concentration in the z -direction yields then an apparent pattern with random correlation length. Since the Cahn-Hilliard equation describes the long-time, long-wavelength properties of the coarsening, the short-time fluctuations of ξ may be an artificial feature of the results. Similarly, the explanation of the presence of an induction time in the $b_0 = 0.48$ M experiments may also be outside the scope of the CH description. The late stage coarsening, however, should be correctly given. $\xi(t)$ is indeed smooth in this regime and, in agreement with the experiments, it shows diffusive behavior ($\xi^2 \sim t$).

We should emphasize that the emergence of a coarsening state is by no means obvious. The rate of the arrival of A and B particles to the front decreases with time (roughly as a_0/\sqrt{t} and b_0/\sqrt{t}) and the front can advance only in the presence of surplus A s. Thus it is also a conceivable scenario that, due to the redissolution process

($A+C \rightarrow Complex$), there is only small concentration of C s in the front with finite (or perhaps even decreasing) correlation length. The selection of a selfsimilar coarsening state is the result of a delicate interplay between the diffusive advance of the front and the reaction-diffusion-aggregation processes within the front.

In conclusion, we studied the coarsening of precipitation patterns in a thin moving reaction front, and our experiments suggest that the asymptotic dynamics of the system may be interpreted as curvature-driven, late-stage coarsening in systems with nonconserved order parameter. The theoretical approach, based on the Cahn-Hilliard equation coupled to reaction-diffusion processes, reproduces all relevant findings observed in experiments, but the question of why selfsimilar coarsening is selected by the dynamics is still to be answered. We believe that, in general, the coupling of reaction fronts with phase separation processes opens a wide range of possibilities for studying new aspects of coarsening and pattern formation, and developing this field is of importance for sub-microscopic technological design.

Acknowledgments

This work has been supported by the Hungarian Academy of Sciences (OTKA No. K 68109, K 68253, and T 72037).

-
- [1] H. K. Henisch, *Periodic precipitation* (Pergamon Press, New York, 1991).
 - [2] W. Lu and C.M. Lieber, *Nat. Mater.* **6**, 841 (2007).
 - [3] I.T. Bensemann, M. Fialkowski, and B.A. Grzybowski, *J. Phys. Chem. B* **109**, 2774 (2005).
 - [4] M.I. Lebedeva, D.G. Vlachos, and M. Tsapatsis, *Phys. Rev. Lett.* **92**, 088301 (2004).
 - [5] O. Giraldo et al., *Nature* **405**, 38 (2000).
 - [6] T. Antal, I. Bena, M. Droz, K. Martens, and Z. Rácz, *Phys. Rev. E* **76**, 046203 (2007).
 - [7] Bena I, Droz M, Lagzi I, Martens K, Rácz Z and Volford A, *Phys. Rev. Lett.* **101** 075701 (2008).
 - [8] L. Gálfi and Z. Rácz, *Phys. Rev. A* **38**, 3151 (1988).
 - [9] T. Antal, M. Droz, J. Magnin, Z. Rácz, and M. Zrinyi, *J. Chem. Phys.* **109**, 9479 (1998).
 - [10] L. Y-E. Koo, R. Kopelman, *J. Stat. Phys.* **65** 893 (1991).
 - [11] C. Léger, F. Argoul, and M. Bazant, *J. Chem. Phys.* **103**, 5841 (1999).
 - [12] C. N. Baroud, F. Okkels, L. Ménétrier, P. Tabeling, *Phys. Rev. E* **67**, 060104 (2003).
 - [13] S.C. Müller, S. Kai, and J. Ross, *J. Phys. Chem.* **86**, 4294 (1982).
 - [14] S. Kai, S.C. Müller, and J. Ross, *J. Phys. Chem.* **87**, 806 (1983).
 - [15] M. Zrinyi, L. Gálfi E. Smidroczi, Z. Rácz, and F. Horkay, *J. Phys. Chem.* **95**, 1618 (1991).
 - [16] R. Sultan, and S. Panjarian, *Physica D* **157**, 241 (2001).
 - [17] R. Sultan, *Phys. Chem. Chem. Phys.* **4**, 1253 (2002).
 - [18] I. Lagzi, P. Pápai, and Z. Rácz, *Chem. Phys. Lett.* **433**, 286 (2007).
 - [19] A. Volford, F. Izsák, M. Ripszám, and I. Lagzi, *Langmuir* **23**, 961 (2007).
 - [20] B.P.J.D. Costello, *Int. J. Unconv. Comput.* **4**, 297 (2008).
 - [21] B.P.J. de Lacy Costello, J. Armstrong, I. Jahan, N.M. Ratcliffe, *Int. J. Nanotechnol. Mol. Comput.* **3**, 26 (2009).
 - [22] K. Binder, *Rep. Prog. Phys.* **50**, 783 (1987).
 - [23] A. J. Bray, *Adv. Phys.* **51**, 481 (2002).
 - [24] For $t \gg 25$ minutes, we observed that the coarsening stopped and the pattern froze. This phenomenon (which is not a finite-size effect since it happens irrespectively of the gel thickness and of the concentration of the inner electrolyte) appears to be rather complex and should be the subject of future studies.
 - [25] T. Antal, M. Droz, J. Magnin, and Z. Rácz, *Phys. Rev. Lett.* **83**, 2880 (1999).
 - [26] In numerical solutions, the noise term was realized by exchanging C s at neighboring sites proportionally to $\sqrt{c}\eta$ where η is a random number uniformly distributed in the interval $[-0.015, 0.015]$.
 - [27] Z. Rácz, *Physica A* **274**, 50 (1999).
 - [28] The calculations were parallelized with CUDA (Compute Unified Device Architecture), the new parallel programming architecture of NVIDIA video cards. A GeForce 8800GTX video card was used to perform computations (2.66 GHz Core2 processor and 4 GB RAM).